

Fully charmed resonance $X(6900)$ and its beauty counterpart

S. S. Agaev,¹ K. Azizi,^{2,3} B. Barsbay,⁴ and H. Sundu⁵

¹*Institute for Physical Problems, Baku State University, Az-1148 Baku, Azerbaijan*

²*Department of Physics, University of Tehran, North Karegar Avenue, Tehran 14395-547, Iran*

³*Department of Physics, Doğuş University, Dudullu-Ümraniye, 34775 Istanbul, Türkiye*

⁴*Division of Optometry, School of Medical Services and Techniques, Doğuş University, 34775 Istanbul, Türkiye*

⁵*Department of Physics Engineering, Istanbul Medeniyet University, 34700 Istanbul, Türkiye*

(ΩDated: April 21, 2023)

The fully heavy scalar tetraquarks $T_{4Q} = QQ\bar{Q}\bar{Q}$, ($Q = c, b$) are explored in the context of QCD sum rule method. We model T_{4Q} as diquark-antidiquark systems composed of pseudoscalar constituents, and calculate their masses $m^{(\prime)}$ and couplings $f^{(\prime)}$ within the two-point sum rule approach. Our results $m = (6928 \pm 50)$ MeV and $m' = (18858 \pm 50)$ MeV for masses of the tetraquarks T_{4c} and T_{4b} prove that they are strong-interaction unstable structures. The full width Γ_{4c} of T_{4c} is evaluated by taking into account its decay channels $T_{4c} \rightarrow J/\psi J/\psi$, $J/\psi\psi'$, $\eta_c\eta_c$, $\eta_c\eta_c(2S)$, and $\eta_c\chi_{c1}(1P)$. The partial widths of these processes depend on strong couplings g_i at vertices $T_{4c}J/\psi J/\psi$, $T_{4c}J/\psi\psi'$ etc., which are computed using QCD three-point sum rule method. The width Γ_{4b} is evaluated from analysis of the decay $T_{4b} \rightarrow \eta_b\eta_b$. Predictions obtained for m and $\Gamma_{4c} = (112 \pm 21)$ MeV are compared with parameters of fully charmed resonances reported by the LHCb, ATLAS, and CMS collaborations. Based on this analysis, we interpret the tetraquark T_{4c} as a candidate to the resonance $X(6900)$. The mass m' and width $\Gamma_{4b} = (94 \pm 28)$ MeV of the fully beauty exotic meson T_{4b} can be used in future experimental investigations of these states.

I. INTRODUCTION

It is known, that existence of exotic states composed of more than three valence partons or bearing unusual quantum numbers is not forbidden by the parton model and first principles of QCD. Phenomenological studies of such multiquark hadrons started almost a half century ago from modeling the nonet of light scalar mesons as $q^2\bar{q}^2$ four-quark states, and analysis of the doubly strange hexaquark structure [1, 2]. Due to collected experimental information and theoretical achievements multiquark hadrons are objects of intensive studies in high energy physics.

Theoretical investigations of multiquark hadrons aimed to elaborate methods to deal with such structures, calculate their parameters, and search for processes to detect them. One of important problems of these studies was a stability of multiquark hadrons against strong and/or electromagnetic decays, because stable particles with long mean lifetimes can be easily observed in various processes. Structures composed of heavy QQ ($Q = c$ or b) diquarks and light antidiquarks are real candidates to such exotic mesons. Thus, it was already demonstrated that compounds $QQ\bar{q}\bar{q}$ may be strong-interaction stable particles provided the ratio m_Q/m_q is large [3–5]. For example, a conclusion about stable nature of the isoscalar axial-vector tetraquark $b\bar{b}\bar{u}\bar{d}$ was made in Ref. [6] confirmed later by other researches [7–9]. Evidently, stable tetraquarks transform to conventional mesons through weak processes, and live considerably longer than other multiquark systems [10–19].

Heavy exotic mesons $QQ\bar{Q}^{(\prime)}\bar{Q}^{(\prime)}$ establish another class of particles, where one may search for stable structures. In the early period of investigations fully heavy tetraquarks were excluded from candidates to stable

particles [3–5]. Studies of last years led to alternative conclusions about features of these structures. It turned out that some of fully heavy tetraquarks may form stable configurations (see Refs. [20, 21], and references therein). Therefore, detailed analyses of four-quark mesons $QQ\bar{Q}^{(\prime)}\bar{Q}^{(\prime)}$ were and remain on agenda of high energy physics.

Experimental data collected by different collaborations inspired and supported theoretical activities in this area [22–26]. In fact, pairs of mesons $J/\psi J/\psi$, $J/\psi\Upsilon(1S)$ and $\Upsilon(1S)\Upsilon(1S)$ produced in pp and $p\bar{p}$ collisions hint at intermediate states $c\bar{c}\bar{c}\bar{c}$, $b\bar{c}\bar{b}\bar{c}$ and $b\bar{b}\bar{b}\bar{b}$ which arise in these processes and decay to couples of heavy conventional mesons.

Recently, the LHCb, ATLAS and CMS collaborations reported about new structures discovered in di- J/ψ and $J/\psi\psi'$ mass distributions [27–29]. The LHCb observed a threshold enhancement in nonresonant di- J/ψ production from 6.2 to 6.8 GeV with center at 6.49 GeV. A narrow peak $X(6900)$ at about 6.9 GeV, and a resonance around 7.2 GeV were seen as well. The ATLAS and CMS experiments detailed information on structures in the region 6.2 – 6.8 GeV and at 7.2 GeV. Thus, ATLAS detected the resonances $X(6200)$, $X(6600)$, and $X(6900)$ in the di- J/ψ , and $X(7300)$ in the $J/\psi\psi'$ channels, respectively. The resonances $X(6600)$, $X(6900)$ and $X(7300)$ were fixed by the CMS collaboration as well.

Analyses made using various methods and models led to interesting, sometimes contradictory, interpretations of the observed fully charmed resonances [20, 21, 30–40]. In fact, the resonance $X(6900)$ was interpreted as a molecule $\chi_{c0}\chi_{c0}$ or/and a tetraquark built of pseudoscalar diquark and antidiquark components [31]. In Ref. [36] $X(6200)$ was assigned to be the ground-level tetraquark state with $J^{PC} = 0^{++}$ or 1^{+-} , whereas

$X(6600)$ was considered as its first radial excitation. Using the relativized Godfrey-Isgur diquark model the authors of Ref. [38] proposed to consider the resonances, starting from $X(6200)$, as the $1S$, $1P/2S$, $1D/2P$, and $2D/3P/4S$ tetraquark states. Similar interpretations in the context of the relativistic quark model were suggested as well [21]. Alternatively, in the framework of the coupled-channel approach a near-threshold state in the di- J/ψ system with $J^{\text{PC}} = 0^{++}$ or $J^{\text{PC}} = 2^{++}$ was interpreted as $X(6200)$ [33]. Coupled-channel effects may also generate a pole structure identified in Ref. [35] with the resonance $X(6900)$.

In our article [20], we carried out rather detailed analysis of fully charmed X_{4c} and beauty X_{4b} scalar four-quark mesons by calculating their masses and current couplings. We modeled X_{4c} and X_{4b} as diquark-antidiquarks built of axial-vector constituents $Q^T C \gamma_\mu Q$ and $\bar{Q} \gamma^\mu C \bar{Q}^T$ (briefly, a tetraquark with a structure $C \gamma_\mu \otimes \gamma^\mu C$), where C is the charge conjugation matrix. Our prediction for the mass $m = (6570 \pm 55)$ MeV of the tetraquark X_{4c} proved that it can decay to $J/\psi J/\psi$, $\eta_c \eta_c$, and $\eta_c \chi_{c1}(1P)$ mesons. The full width of X_{4c} was computed using these decay modes and found equal to $\Gamma_{4c} = (110 \pm 21)$ MeV. Comparison of these results with available data allowed us to consider X_{4c} as a candidate to the resonance $X(6600)$. We also argued that $X(7300)$ may be considered as $2S$ excitation of the resonance $X(6600)$. In Ref. [20], we calculated the mass of the fully beauty scalar state X_{4b} as well. It turned out that, its mass $m' = (18540 \pm 50)$ MeV is below the $\eta_b \eta_b$ threshold, and hence X_{4b} is strong-interaction stable particle. This tetraquark is observable neither in $\eta_b \eta_b$ nor $\Upsilon(1S) \Upsilon(1S)$ mass distributions: Transformation of X_{4b} to ordinary mesons may proceed through weak leptonic and nonleptonic processes.

In the present work, we continue our explorations of the LHCb-ATLAS-CMS resonances in the context of the diquark-antidiquark model. We compute parameters of the scalar $J^{\text{PC}} = 0^{++}$ state T_{4c} built of pseudoscalar diquark components, i. e., a tetraquark with $C \otimes C$ type internal organization. We calculate the mass and full width of T_{4c} , and confront our results with experimental data for the fully charmed X resonances. We investigate also its beauty counterpart T_{4b} to determine the mass and width of this state.

The current paper is organized in the following manner: In Section II, we calculate the mass and current coupling of the tetraquarks T_{4c} and T_{4b} . Strong decays of T_{4c} to different charmonium pairs are studied in Secs. III and IV. In Sec. III, we consider decays of T_{4c} to mesons $J/\psi J/\psi$, and $J/\psi \psi'$. The processes $X_{4c} \rightarrow \eta_c \eta_c$, $\eta_c \eta_c(2S)$ and $\eta_c \chi_{c1}(1P)$ are analyzed in Sec. IV. Here, we determine also the full width of T_{4c} . The width of the decay $T_{4b} \rightarrow \eta_b \eta_b$ is computed in Sec. V. Last section is reserved for discussion of results and contains our concluding notes.

II. MASS AND CURRENT COUPLING OF THE TETRAQUARKS T_{4c} AND T_{4b}

Here, we calculate the masses $m^{(i)}$ and current couplings $f^{(i)}$ of the tetraquarks T_{4c} and T_{4b} in the context of the QCD two-point sum rule approach [41, 42]. To this end, we consider the correlation function

$$\Pi(p) = i \int d^4x e^{ipx} \langle 0 | \mathcal{T} \{ J(x) J^\dagger(0) \} | 0 \rangle, \quad (1)$$

where, \mathcal{T} is the time-ordered product of two currents, and $J(x)$ is the interpolating currents for these states. We treat the tetraquarks T_{4c} and T_{4b} as states built of pseudoscalar diquark $Q^T C Q$ and pseudoscalar antidiquark $\bar{Q} C \bar{Q}^T$. Then relevant interpolating current is defined by the expression

$$J(x) = Q_a^T(x) C Q_b(x) \bar{Q}_a(x) C \bar{Q}_b^T(x), \quad (2)$$

where a , and b are color indices, and $Q(x)$ is either c or b quark field. The current $J(x)$ describes the diquark-antidiquark state with quantum numbers $J^{\text{PC}} = 0^{++}$.

Below, we write down formulas for the tetraquark T_{4c} , which can be readily extended to the case of T_{4b} . The physical side of the sum rule $\Pi^{\text{Phys}}(p)$ can be found from Eq. (1) by inserting a complete set of intermediate states with quark content and spin-parities of the tetraquark T_{4c} , and carrying out integration over x . As a result, we get

$$\Pi^{\text{Phys}}(p) = \frac{\langle 0 | J | T_{4c}(p) \rangle \langle T_{4c}(p) | J^\dagger | 0 \rangle}{m^2 - p^2} + \dots, \quad (3)$$

where p is four-momentum of $T_{4c}(p)$. The ellipses in Eq. (3) stand for contributions of higher resonances and continuum states.

The correlation function $\Pi^{\text{Phys}}(p)$ can be rewritten in terms of the tetraquarks' parameters through

$$\langle 0 | J | T_{4c}(p) \rangle = f m, \quad (4)$$

which gives

$$\Pi^{\text{Phys}}(p) = \frac{f^2 m^2}{m^2 - p^2} + \dots \quad (5)$$

The correlator $\Pi^{\text{Phys}}(p)$ has simple Lorentz structure which is proportional to \mathbf{I} . Therefore, an invariant amplitude $\Pi^{\text{Phys}}(p^2)$ required to derive the sum rules is equal to rhs of Eq. (5).

The counterpart of $\Pi^{\text{Phys}}(p^2)$, i.e., the invariant amplitude $\Pi^{\text{OPE}}(p^2)$ evaluated by employing heavy quark propagators establishes the QCD side of the sum rule. The function $\Pi^{\text{OPE}}(p^2)$ should be extracted from a term $\sim \mathbf{I}$ in the correlator $\Pi^{\text{OPE}}(p)$. The latter is calculated in the operator product expansion (OPE) with some fixed accuracy and contains only a component proportional to \mathbf{I} .

We compute $\Pi^{\text{OPE}}(p)$ by substituting the current $J(x)$ into Eq. (1), contracting relevant quark fields, and replacing them by the heavy quark propagators, and find

$$\begin{aligned} \Pi^{\text{OPE}}(p) = & i \int d^4x e^{ipx} \left\{ \text{Tr} \left[\tilde{S}_c^{b'b}(-x) S_c^{a'a}(-x) \right] \right. \\ & \times \left[\text{Tr} \left[\tilde{S}_c^{aa'}(x) S_c^{bb'}(x) \right] + \text{Tr} \left[\tilde{S}_c^{ba'}(x) \right. \right. \\ & \times \left. \left. S_c^{ab'}(x) \right] \right] + \text{Tr} \left[\tilde{S}_c^{a'b}(-x) S_c^{b'a}(-x) \right] \\ & \times \left. \left[\text{Tr} \left[\tilde{S}_c^{ba'}(x) S_c^{ab'}(x) \right] + \text{Tr} \left[\tilde{S}_c^{aa'}(x) S_c^{bb'}(x) \right] \right] \right\}. \end{aligned} \quad (6)$$

Here,

$$\tilde{S}_c(x) = C S_c^T(x) C, \quad (7)$$

where $S_c(x)$ is the c -quark propagator. Explicit expression of the heavy quark propagator $S_Q(x)$ can be found in Refs. [20, 43].

At the next stage of analysis, we equate the amplitudes $\Pi^{\text{Phys}}(p^2)$ and $\Pi^{\text{OPE}}(p^2)$, apply the Borel transformation to suppress effects of higher resonances and continuum state, and make use of the assumption on quark-hadron duality to subtract these terms from the physical side of the sum rule equality. After some trivial manipulations, we derive the following sum rules for the mass m and current coupling f of the tetraquark $T_{4c}(p)$:

$$m^2 = \frac{\Pi'(M^2, s_0)}{\Pi(M^2, s_0)}, \quad (8)$$

and

$$f^2 = \frac{e^{m^2/M^2}}{m^2} \Pi(M^2, s_0), \quad (9)$$

where $\Pi'(M^2, s_0) = d\Pi(M^2, s_0)/d(-1/M^2)$. In Eqs. (8) and (9) the function $\Pi(M^2, s_0)$ is the amplitude $\Pi^{\text{OPE}}(p^2)$ after the Borel transformation and continuum subtraction procedures. It depends on the Borel M^2 and continuum subtraction s_0 parameters, which appear in the sum rule equality after corresponding operations.

Our analysis demonstrates that the function $\Pi(M^2, s_0)$ has the form

$$\Pi(M^2, s_0) = \int_{16m_c^2}^{s_0} ds \rho^{\text{OPE}}(s) e^{-s/M^2}, \quad (10)$$

where $\rho^{\text{OPE}}(s)$ is a two-point spectral density determined as an imaginary part of the invariant amplitude $\Pi^{\text{OPE}}(p^2)$. The function $\rho^{\text{OPE}}(s)$ consists of a perturbative term $\rho^{\text{pert.}}(s)$ and a dimension-4 nonperturbative contribution $\sim \langle \alpha_s G^2/\pi \rangle$. Explicit expression of $\rho^{\text{OPE}}(s)$ is rather lengthy and we do not write down it here.

In the case under discussion, $\Pi^{\text{OPE}}(p)$ depends only on c -quark propagators. The propagator $S_c(x)$ apart from a perturbative term, contains also components linear and quadratic in gluon field strength. It does not depend on

light quark and mixed quark-gluon condensates. Therefore, for numerical analysis of the sum rules Eqs. (8) and (9), we need the masses of c and b quarks, as well as the gluon vacuum condensate $\langle \alpha_s G^2/\pi \rangle$: Values of these parameters are presented below

$$\begin{aligned} m_c &= (1.27 \pm 0.02) \text{ GeV}, \\ m_b &= 4.18_{-0.02}^{+0.03} \text{ GeV}, \\ \langle \frac{\alpha_s G^2}{\pi} \rangle &= (0.012 \pm 0.004) \text{ GeV}^4. \end{aligned} \quad (11)$$

One should also fix working regions for parameters M^2 and s_0 . The M^2 and s_0 have to satisfy constraints imposed on $\Pi(M^2, s_0)$ by a pole contribution (PC) and convergence of the operator product expansion. To evaluate PC, we employ the expression

$$\text{PC} = \frac{\Pi(M^2, s_0)}{\Pi(M^2, \infty)}, \quad (12)$$

and require fulfillment of the constraint $\text{PC} \geq 0.5$.

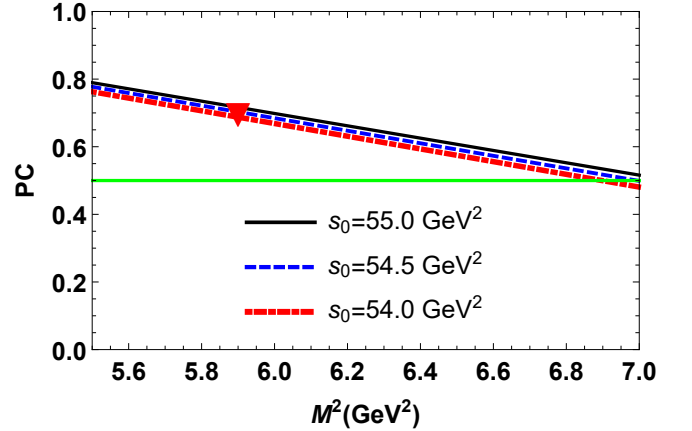


FIG. 1: The pole contribution PC as a function of the Borel parameter M^2 at different s_0 . The limit $\text{PC} = 0.5$ is plotted by the horizontal line. The red triangle shows the point, where the mass m of the tetraquark T_{4c} has been extracted from the sum rule.

Because, the sum rules for m and f depend only on a nonperturbative term $\sim \langle \alpha_s G^2/\pi \rangle$, the pole contribution becomes an important criterium in the choice of M^2 and s_0 . We demand also a stability of extracted observables under variations of the Borel and continuum subtraction parameters. In fact, M^2 and s_0 are the auxiliary parameters of computations, and physical quantities should not depend on M^2 and s_0 . In real analysis however, m and f bear residual dependence on these parameters. Hence, a maximal stability of m and f under variations of M^2 and s_0 is among important constraints in the choice of relevant working intervals. The prevalence of a perturbative contribution over nonperturbative one is also required condition.

By employing PC one can fix the higher limit of the Borel parameter M^2 . The lower border for M^2 is

found from the restriction imposed on the nonperturbative term. Two values of M^2 determined by this manner limit the region where M^2 can be changed. Computations demonstrate that windows

$$M^2 \in [5.5, 7] \text{ GeV}^2, \quad s_0 \in [54, 55] \text{ GeV}^2, \quad (13)$$

meet all necessary constraints in the case of the tetraquark T_{4c} . Thus, at $M^2 = 5.5 \text{ GeV}^2$ and $M^2 = 7 \text{ GeV}^2$ the pole contribution equals to 0.78 and 0.51, respectively. At the minimum of $M^2 = 5.5 \text{ GeV}^2$, a contribution of the nonperturbative term is negative and forms 14% of the correlation function.

In Fig. 1, we plot PC as a function of M^2 at different s_0 , in order to show dynamics of the pole contribution. As is seen, it exceeds 0.5 for all values of the parameters

M^2 and s_0 from Eq. (13).

The mass m and current coupling f of the tetraquark T_{4c} are calculated as their mean values averaged over the regions Eq. (13). Our results for m and f are

$$\begin{aligned} m &= (6928 \pm 50) \text{ MeV}, \\ f &= (2.06 \pm 0.14) \times 10^{-2} \text{ GeV}^4. \end{aligned} \quad (14)$$

These predictions correspond to sum rules' results at the point $M^2 = 5.9 \text{ GeV}^2$ and $s_0 = 54.5 \text{ GeV}^2$, where the pole contribution is $\text{PC} \approx 0.7$ (see, Fig. 1). This fact ensures dominance of PC in these results, and ground-state nature of the exotic meson T_{4c} . The mass m of the tetraquark T_{4c} is plotted in Fig. 2 as a function of M^2 and s_0 .

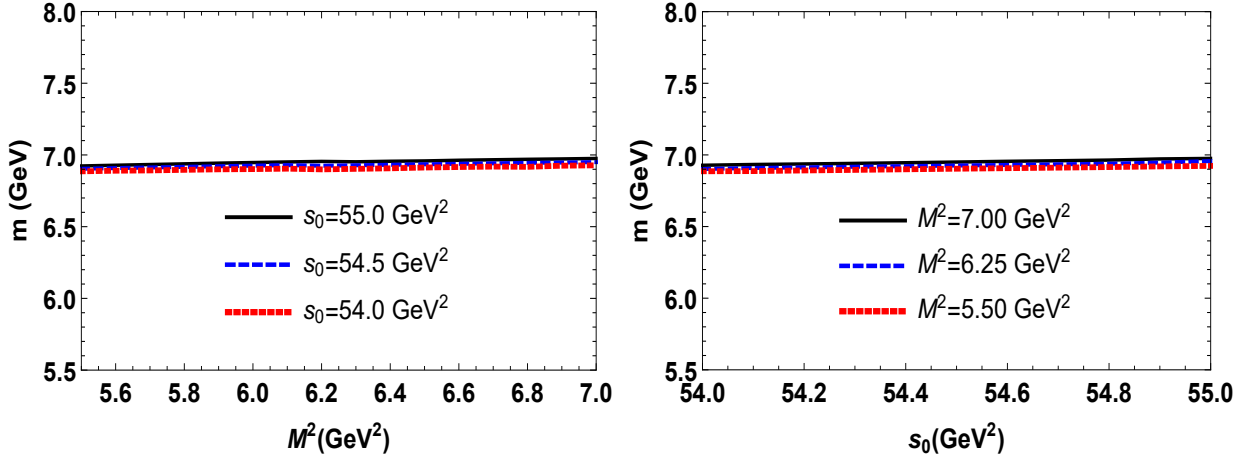


FIG. 2: Mass of the tetraquark T_{4c} as a function of the Borel parameter M^2 (left), and as a function of the continuum threshold s_0 (right).

In the case of the tetraquark T_{4b} analysis performed to choose the working regions for the Borel and continuum subtraction parameters gives

$$\begin{aligned} M^2 &\in [17.5, 18.5] \text{ GeV}^2, \\ s_0 &\in [380, 385] \text{ GeV}^2. \end{aligned} \quad (15)$$

Here, the PC varies within the interval

$$0.64 \geq \text{PC} \geq 0.58. \quad (16)$$

The dimension-4 term constitutes -2.2% of the result at $M^2 = 17.5 \text{ GeV}^2$. The mass and current coupling of the fully beauty tetraquark T_{4b} are equal to

$$\begin{aligned} m' &= (18858 \pm 50) \text{ MeV}, \\ f' &= (9.54 \pm 0.71) \times 10^{-2} \text{ GeV}^4. \end{aligned} \quad (17)$$

Behavior of m' as a function of M^2 and s_0 is shown in Fig. 3.

The mass m of the tetraquark T_{4c} is in excellent agreement with the mass of the resonance $X(6900)$ measured by the CMS collaboration. It is also compatible with LHCb and ATLAS data though slightly exceeds them. But for detailed comparison with available data, and more reliable conclusions on nature of T_{4c} , we have to estimate its full width.

The diquark-antidiquark state T_{4b} with $C \otimes C$ structure and mass $m' = 18858 \text{ MeV}$ is above $\eta_b \eta_b$ but below $\Upsilon(1S) \Upsilon(1S)$ thresholds. Consequently, it decays to a $\eta_b \eta_b$ pair and should be searched for in invariant mass distributions of these mesons.

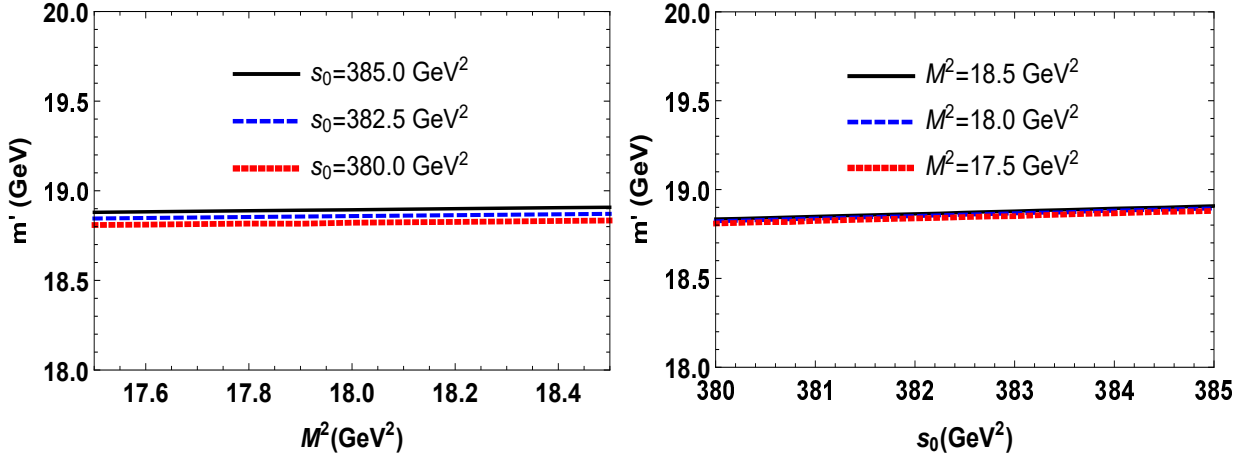


FIG. 3: The same as in Fig. 2, but for the mass m' of the tetraquark T_{4b} .

III. DECAYS $T_{4c} \rightarrow J/\psi J/\psi$ AND $T_{4c} \rightarrow J/\psi \psi'$

The prediction for the mass of the diquark-antidiquark system with structure $C \otimes C$ permits us to determine the kinematically allowed decay modes of T_{4c} . The mass $m = 6928$ MeV of this tetraquark exceeds the two-meson $J/\psi J/\psi$ and $J/\psi \psi'$ thresholds. The m satisfies also the kinematical restrictions for productions of $\eta_c \eta_c$ and $\eta_c \eta_c(2S)$ pairs. T_{4c} can decay to conventional $\eta_c \chi_{c1}(1P)$ mesons as well. The first four decays are S -wave processes, whereas $T_{4c} \rightarrow \eta_c \chi_{c1}(1P)$ is P -wave decay channel.

We start our studies from investigation of the processes $J/\psi J/\psi$ and $J/\psi \psi'$. The three-point sum rules for the strong form factors $g_1(q^2)$ and $g_1^*(q^2)$ which describe interaction of particles at vertices $T_{4c} J/\psi J/\psi$ and $T_{4c} J/\psi \psi'$ respectively, can be extracted from analysis of the correlation function

$$\Pi_{\mu\nu}(p, p') = i^2 \int d^4x d^4y e^{ip'y} e^{-ipx} \langle 0 | \mathcal{T} \{ J_\mu^\psi(y) \times J_\nu^\psi(0) J^\dagger(x) \} | 0 \rangle, \quad (18)$$

where the current $J(x)$ is defined by Eq. (2), and $J_\mu^\psi(x)$ is the interpolating currents for the mesons J/ψ and ψ'

$$J_\mu^\psi(x) = \bar{c}_i(x) \gamma_\mu c_i(x), \quad (19)$$

where $i = 1, 2, 3$ are the color indices.

We apply usual recipes of the sum rule method and express the correlation function $\Pi_{\mu\nu}(p, p')$ in terms of physical parameters of particles. Because the tetraquark T_{4c} can decay both to $J/\psi J/\psi$ and $J/\psi \psi'$ pairs, we isolate in $\Pi_{\mu\nu}(p, p')$ contributions of the particles J/ψ and ψ' from effects of higher resonances and continuum states. Then,

for the physical side of the sum rule $\Pi_{\mu\nu}^{\text{Phys}}(p, p')$, we get

$$\begin{aligned} \Pi_{\mu\nu}^{\text{Phys}}(p, p') &= \frac{\langle 0 | J_\mu^\psi | J/\psi(p') \rangle \langle 0 | J_\nu^\psi | J/\psi(q) \rangle}{p'^2 - m_1^2} \frac{\langle 0 | J_\nu^\psi | J/\psi(q) \rangle}{q^2 - m_1^2} \\ &\times \langle J/\psi(p') J/\psi(q) | T_{4c}(p) \rangle \frac{\langle T_{4c}(p) | J^\dagger | 0 \rangle}{p^2 - m^2} \\ &+ \frac{\langle 0 | J_\mu^\psi | \psi(p') \rangle \langle 0 | J_\nu^\psi | J/\psi(q) \rangle}{p'^2 - m_1^{*2}} \frac{\langle 0 | J_\nu^\psi | J/\psi(q) \rangle}{q^2 - m_1^2} \\ &\times \langle \psi(p') J/\psi(q) | T_{4c}(p) \rangle \frac{\langle T_{4c}(p) | J^\dagger | 0 \rangle}{p^2 - m^2} + \dots, \quad (20) \end{aligned}$$

with m_1 and m_1^* being the masses of J/ψ and ψ' mesons. The 4-momentum of the tetraquark T_{4c} is p , whereas in the first term momenta of the J/ψ mesons are p' and $q = p - p'$, respectively. In the second term in Eq. (20), ψ' and J/ψ have the momenta p' and q .

The function $\Pi_{\mu\nu}^{\text{Phys}}(p, p')$ can be rewritten by using the matrix elements of the tetraquark T_{4c} , and mesons J/ψ and ψ' . The matrix element of T_{4c} is given by Eq. (4), whereas for $\langle 0 | J_\mu^\psi | J/\psi(p) \rangle$ and $\langle 0 | J_\mu^\psi | \psi'(p) \rangle$, we utilize

$$\begin{aligned} \langle 0 | J_\mu^\psi | J/\psi(p) \rangle &= f_1 m_1 \varepsilon_\mu(p), \\ \langle 0 | J_\mu^\psi | \psi'(p) \rangle &= f_1^* m_1^* \tilde{\varepsilon}_\mu(p), \end{aligned} \quad (21)$$

where f_1 , f_1^* , and ε_μ , $\tilde{\varepsilon}$ are the decay constants and polarization vectors of J/ψ and ψ' , respectively.

We model the vertices in the following form

$$\begin{aligned} \langle J/\psi(p') J/\psi(q) | T_{4c}(p) \rangle &= g_1(q^2) [q \cdot p' \varepsilon^*(p') \cdot \varepsilon^*(q) \\ &- q \cdot \varepsilon^*(p') p' \cdot \varepsilon^*(q)], \end{aligned} \quad (22)$$

and

$$\begin{aligned} \langle \psi(p') J/\psi(q) | T_{4c}(p) \rangle &= g_1^*(q^2) [q \cdot p' \tilde{\varepsilon}^*(p') \cdot \varepsilon^*(q) \\ &- q \cdot \tilde{\varepsilon}^*(p') p' \cdot \varepsilon^*(q)]. \end{aligned} \quad (23)$$

Having used these matrix elements and carried out simple calculations, we find for $\Pi_{\mu\nu}^{\text{Phys}}(p, p')$

$$\begin{aligned} \Pi_{\mu\nu}^{\text{Phys}}(p, p') &= g_1(q^2) \frac{f m f_1^2 m_1^2}{(p^2 - m^2)(p'^2 - m_1^2)(q^2 - m_1^2)} \\ &\times \left[\frac{1}{2} (m^2 - m_1^2 - q^2) g_{\mu\nu} - q_\mu p'_\nu \right] + \\ &+ g_1^*(q^2) \frac{f m f_1 m_1 f_1^* m_1^*}{(p^2 - m^2)(p'^2 - m_1^{*2})(q^2 - m_1^2)} \\ &\times \left[\frac{1}{2} (m^2 - m_1^{*2} - q^2) g_{\mu\nu} - q_\mu p'_\nu \right] + \dots, \end{aligned} \quad (24)$$

where dots stand for contributions of higher resonances and continuum states. The correlator Eq. (24) contains different Lorentz structures, which can be employed to determine the sum rules for $g_1(q^2)$ and $g_1^*(q^2)$. We work with the structures $\sim g_{\mu\nu}$ and denote the relevant invariant amplitudes by $\Pi_1^{\text{Phys}}(p^2, p'^2, q^2)$ and $\Pi_2^{\text{Phys}}(p^2, p'^2, q^2)$, respectively. Then, a total amplitude $\Pi^{\text{Phys}}(p^2, p'^2, q^2)$ is equal to a sum of functions $\Pi_{1,2}^{\text{Phys}}(p^2, p'^2, q^2)$. The Borel transformations of $\Pi^{\text{Phys}}(p^2, p'^2, q^2)$ over p^2 and p'^2 give

$$\begin{aligned} \mathcal{B}\Pi^{\text{Phys}}(p^2, p'^2, q^2) &= g_1(q^2) f m f_1^2 m_1^2 \\ &\times \frac{m^2 - m_1^2 - q^2}{2(q^2 - m_1^2)} e^{-m^2/M_1^2} e^{-m_1^2/M_2^2} \\ &+ g_1^*(q^2) f m f_1 m_1 f_1^* m_1^* \frac{m^2 - m_1^{*2} - q^2}{2(q^2 - m_1^2)} \\ &\times e^{-m^2/M_1^2} e^{-m_1^{*2}/M_2^2} + \dots \end{aligned} \quad (25)$$

The correlation function $\Pi_{\mu\nu}(p, p')$ expressed in terms of the c -quark propagators establishes the QCD side of the sum rule

$$\begin{aligned} \Pi_{\mu\nu}^{\text{OPE}}(p, p') &= 2i^2 \int d^4x d^4y e^{ip'y} e^{-ipx} \\ &\times \left\{ \text{Tr} \left[\gamma_\mu S_c^{ib}(y-x) \tilde{S}_c^{ja}(-x) \gamma_\nu \tilde{S}_c^{bj}(x) S_c^{ai}(x-y) \right] \right. \\ &\left. + \text{Tr} \left[\gamma_\mu S_c^{ia}(y-x) \tilde{S}_c^{jb}(-x) \gamma_\nu \tilde{S}_c^{bj}(x) S_c^{ai}(x-y) \right] \right\}. \end{aligned} \quad (26)$$

The invariant amplitude $\Pi^{\text{OPE}}(p^2, p'^2, q^2)$ which corresponds to the term $\sim g_{\mu\nu}$ in Eq. (26) forms the QCD side of the sum rules. By equating the double Borel transforms of the amplitudes $\Pi^{\text{OPE}}(p^2, p'^2, q^2)$ and $\Pi^{\text{Phys}}(p^2, p'^2, q^2)$, and carrying out the continuum subtraction, one can find the sum rule for the form factors $g_1(q^2)$ and $g_1^*(q^2)$.

After the Borel transformation and continuum subtraction, $\Pi^{\text{OPE}}(p^2, p'^2, q^2)$ can be written down in terms of the spectral density $\rho(s, s', q^2)$ determined as a relevant imaginary part of $\Pi_{\mu\nu}^{\text{OPE}}(p, p')$

$$\begin{aligned} \Pi(\mathbf{M}^2, \mathbf{s}_0, q^2) &= \int_{16m_c^2}^{s_0} ds \int_{4m_c^2}^{s'_0} ds' \rho(s, s', q^2) \\ &\times e^{-s/M_1^2} e^{-s'/M_2^2}. \end{aligned} \quad (27)$$

Parameters	Values (in MeV)
$m_1[m_{J/\psi}]$	3096.900 ± 0.006
$f_1[f_{J/\psi}]$	409 ± 15
$m_1^*[m_{\psi'}]$	3686.10 ± 0.06
$f_1^*[f_{\psi'}]$	279 ± 8
$m_2[m_{\eta_c}]$	2983.9 ± 0.4
$f_2[f_{\eta_c}]$	398.1 ± 1.0
$m_2^*[m_{\eta_c(2S)}]$	3637.5 ± 1.1
$f_2^*[f_{\eta_c(2S)}]$	331
$m_3[m_{\chi_{c1}}]$	3510.67 ± 0.05
$f_3[f_{\chi_{c1}}]$	344 ± 27
$m_4[m_{\eta_b}]$	9398.7 ± 2.0
$f_4[f_{\eta_b}]$	724 ± 12

TABLE I: Masses and decay constants of the various charmonia and bottomonium η_b which have been used in numerical computations.

Here, $\mathbf{M}^2 = (M_1^2, M_2^2)$ and $\mathbf{s}_0 = (s_0, s'_0)$ are the Borel and continuum threshold parameters, respectively. The pair of parameters (M_1^2, s_0) corresponds to the tetraquark channel, the pair (M_2^2, s'_0) – to the J/ψ or ψ' channels.

To extract the sum rules for $g_1(q^2)$ and $g_1^*(q^2)$, at the first stage of analysis, we fix the continuum subtraction parameter as $4m_c^2 < s'_0 < m_1^{*2}$. By this way, we include the second term in Eq. (25) into higher resonances and continuum states. This scheme is the standard "ground-state+continuum" approach, when the physical side of the sum rule contains a contribution coming only from ground-state particles. Then, it is not difficult to derive the sum rule for the form factor $g_1(q^2)$

$$\begin{aligned} g_1(q^2) &= \frac{2}{f m f_1^2 m_1^2} \frac{q^2 - m_1^2}{m^2 - m_1^2 - q^2} \\ &\times e^{m^2/M_1^2} e^{m_1^2/M_2^2} \Pi(\mathbf{M}^2, \mathbf{s}_0, q^2). \end{aligned} \quad (28)$$

Here, for simplicity, we do not show explicitly \mathbf{M}^2 and \mathbf{s}_0 as arguments of the function $g_1(q^2)$.

At the next phase of calculations, we choose $s'_0 > m_1^{*2}$, and include also the second term in Eq. (25) into consideration. This is "ground-state + excited state+continuum" scheme, which can be used to determine the form factor $g_1^*(q^2)$. Afterwards, by employing results obtained for $g_1(q^2)$ one can determine $g_1^*(q^2)$.

The form factors $g_1(q^2)$ and $g_1^*(q^2)$ depend on the masses and decay constants of the tetraquark T_{4c} and mesons J/ψ and ψ' , which are input parameters in calculations. Their numerical values are collected in Table I. Additionally, this table contains the parameters of the η_c , $\eta_c(2S)$, $\chi_{c1}(1P)$, and η_b mesons which are necessary to explore decay modes of T_{4c} and T_{4b} . For the masses of the particles, we utilize information from Ref. [44]. For decay constant of the meson J/ψ , we employ the experimental value reported in Ref. [45]. As f_{η_c} and f_{η_b} , we use results of QCD lattice simulations [46, 47], whereas for $f_{\chi_{c1}}$ – the sum rule prediction from Ref. [48].

To perform numerical computations, we also have to choose the working regions for the parameters \mathbf{M}^2 and s_0 . They should meet standard constraints of sum rule calculations, which have been discussed in Sec. II. For M_1^2 and s_0 which are actual for the X_{4c} channel, we employ the working regions Eq. (13). The parameters (M_2^2 , s'_0) for the J/ψ channel are changed within limits

$$M_2^2 \in [4, 5] \text{ GeV}^2, \quad s'_0 \in [12, 13] \text{ GeV}^2. \quad (29)$$

In the second phase of analysis, we use

$$M_2^2 \in [4, 5] \text{ GeV}^2, \quad s'_0 \in [15, 16] \text{ GeV}^2. \quad (30)$$

The sum rule method gives reliable predictions in the deep-Euclidean region $q^2 < 0$. Therefore, it is convenient to introduce a new variable $Q^2 = -q^2$ and denote the obtained function by $g_1(Q^2)$. The range of Q^2 analyzed by the sum rule method covers the interval $Q^2 = 1 - 10 \text{ GeV}^2$. Results of calculations are plotted in Fig. 4.

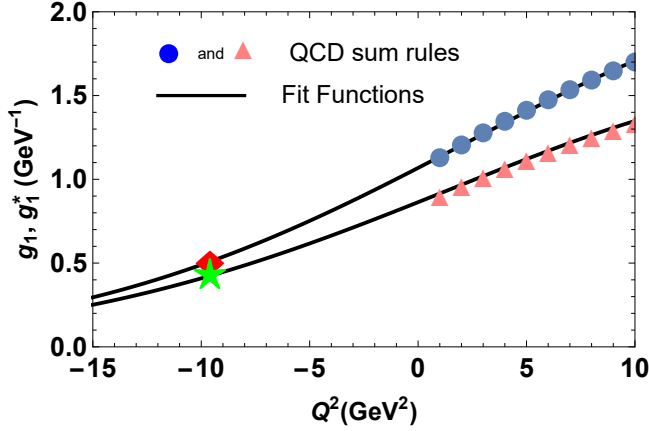


FIG. 4: The sum rule predictions and fit functions for the form factors $g_1(Q^2)$ (upper line) and $g_1^*(Q^2)$ (lower line). The red diamond and green star denote the point $Q^2 = -m_1^2$, where the strong couplings g_1 and g_1^* are evaluated.

But the width of the decay $T_{4c} \rightarrow J/\psi J/\psi$ is determined by the form factor $g_1(q^2)$ at the mass shell $q^2 = m_1^2$. Stated differently, one has to find $g_1(Q^2 = -m_1^2)$. To avoid this problem, we use a fit function $\mathcal{G}_1(Q^2)$, which at momenta $Q^2 > 0$ gives the same values as the sum rule calculations, but can be extrapolated to the region of $Q^2 < 0$. To this end, we employ functions $\mathcal{G}_i^{(*)}(Q^2)$

$$\mathcal{G}_i^{(*)}(Q^2) = \mathcal{G}_i^{0(*)} \exp \left[c_i^{1(*)} \frac{Q^2}{m^2} + c_i^{2(*)} \left(\frac{Q^2}{m^2} \right)^2 \right], \quad (31)$$

with parameters $\mathcal{G}_i^{0(*)}$, $c_i^{1(*)}$ and $c_i^{2(*)}$. Calculations demonstrate that $\mathcal{G}_1^0 = 1.07 \text{ GeV}^{-1}$, $c_1^1 = 2.99$, and $c_1^2 = -3.57$ give a nice agreement with the sum rules data for $g_1(Q^2)$ shown in Fig. 4.

At the mass shell $q^2 = m_1^2$ the function $\mathcal{G}_1(Q^2)$ is equal to

$$g_1 \equiv \mathcal{G}_1(-m_1^2) = (5.1 \pm 1.1) \times 10^{-1} \text{ GeV}^{-1}. \quad (32)$$

Partial width of the process $T_{4c} \rightarrow J/\psi J/\psi$ can be evaluated by employing the following expression

$$\Gamma[T_{4c} \rightarrow J/\psi J/\psi] = g_1^2 \frac{\lambda}{8\pi} \left(\frac{m_1^4}{m^2} + \frac{2\lambda^2}{3} \right), \quad (33)$$

where $\lambda = \lambda(m, m_1, m_1)$ and

$$\lambda(a, b, c) = \frac{\sqrt{a^4 + b^4 + c^4 - 2(a^2b^2 + a^2c^2 + b^2c^2)}}{2a}. \quad (34)$$

Then it is easy to find that

$$\Gamma[T_{4c} \rightarrow J/\psi J/\psi] = (56 \pm 18) \text{ MeV}. \quad (35)$$

The decay $T_{4c} \rightarrow J/\psi \psi'$ can be explored in accordance with a scheme described above. In this case, the extrapolating function $\mathcal{G}_1^*(Q^2)$ has the parameters $\mathcal{G}_1^{0*} = 0.86 \text{ GeV}^{-1}$, $c_1^{1*} = 2.86$, and $c_1^{2*} = -3.47$. The sum rule predictions for the coupling $g_1^*(q^2)$, as well as the function $\mathcal{G}_1^*(Q^2)$ are depicted in Fig. 4. One can be convinced in a reasonable agreement between the sum rules data and $\mathcal{G}_1^*(Q^2)$.

The strong coupling g_1^* is calculated at the mass shell $q^2 = m_1^2$

$$g_1^* \equiv \mathcal{G}_1^*(-m_1^2) = (4.2 \pm 1.0) \times 10^{-1} \text{ GeV}^{-1}. \quad (36)$$

The width of the process is found by means of Eq. (33) with the following replacements $g_1 \rightarrow g_1^*$, $\lambda \rightarrow \lambda(m, m_1^*, m_1)$, and $m_1^4 \rightarrow m_1^2 m_1^{*2}$ which leads to the result

$$\Gamma[T_{4c} \rightarrow J/\psi \psi'] = (15 \pm 5) \text{ MeV}. \quad (37)$$

Essential parameters of these decays are shown in Table II.

IV. PROCESSES $T_{4c} \rightarrow \eta_c \eta_c$; $\eta_c \eta_c(2S)$; $\eta_c \chi_{c1}(1P)$

The decays $T_{4c} \rightarrow \eta_c \eta_c$ and $T_{4c} \rightarrow \eta_c \eta_c(2S)$ can be explored in a similar way. The strong couplings g_2 and g_2^* which correspond to the vertices $T_{4c} \eta_c \eta_c$ and $T_{4c} \eta_c \eta_c(2S)$ can be extracted from the correlation function

$$\begin{aligned} \Pi(p, p') &= i^2 \int d^4x d^4y e^{ip'y} e^{-ipx} \langle 0 | \mathcal{T} \{ J^{\eta_c}(y) \\ &\times J^{\eta_c}(0) J^\dagger(x) \} | 0 \rangle, \end{aligned} \quad (38)$$

where the current $J^{\eta_c}(x)$ is

$$J^{\eta_c}(x) = \bar{c}_i(x) i \gamma_5 c_i(x). \quad (39)$$

Separating the ground-level and first excited state contributions from effects of higher resonances and continuum

states, we write the correlation function (38) in the following form

$$\begin{aligned} \Pi^{\text{Phys}}(p, p') &= \frac{\langle 0 | J^{\eta_c} | \eta_c(p') \rangle}{p'^2 - m_2^2} \frac{\langle 0 | J^{\eta_c} | \eta_c(q) \rangle}{q^2 - m_2^2} \\ &\times \langle \eta_c(p') \eta_c(q) | T_{4c}(p) \rangle \frac{\langle T_{4c}(p) | J^\dagger | 0 \rangle}{p^2 - m^2} \\ &+ \frac{\langle 0 | J^{\eta_c} | \eta_c(2S)(p') \rangle}{p'^2 - m_2^{*2}} \frac{\langle 0 | J^{\eta_c} | \eta_c(q) \rangle}{q^2 - m_2^2} \\ &\times \langle \eta_c(2S)(p') \eta_c(q) | T_{4c}(p) \rangle \frac{\langle T_{4c}(p) | J^\dagger | 0 \rangle}{p^2 - m^2} + \dots, \end{aligned} \quad (40)$$

where m_2 and m_2^* are the masses of the η_c and $\eta_c(2S)$ mesons. The matrix elements of scalar and two pseudoscalar particles' vertices are modeled in the form

$$\begin{aligned} \langle \eta_c(p') \eta_c(q) | T_{4c}(p) \rangle &= g_2(q^2) p \cdot p', \\ \langle \eta_c(2S)(p') \eta_c(q) | T_{4c}(p) \rangle &= g_2^*(q^2) p \cdot p'. \end{aligned} \quad (41)$$

To express the correlator $\Pi^{\text{Phys}}(p, p')$ in terms of physical parameters of the particles T_{4c} , η_c , and $\eta_c(2S)$, we use the matrix element Eq. (4) and

$$\langle 0 | J^{\eta_c} | \eta_c \rangle = \frac{f_2 m_2^2}{2m_c}, \quad \langle 0 | J^{\eta_c} | \eta_c(2S) \rangle = \frac{f_2^* m_2^{*2}}{2m_c}, \quad (42)$$

with f_2 and f_2^* being the decay constants of the mesons η_c and $\eta_c(2S)$, respectively. The correlation function $\Pi^{\text{Phys}}(p, p')$ then takes the form

$$\begin{aligned} \Pi^{\text{Phys}}(p, p') &= \frac{g_2(q^2) f m f_2^2 m_2^4}{8m_c^2 (p^2 - m^2) (p'^2 - m_2^2)} \\ &\times \frac{m^2 + m_2^2 - q^2}{q^2 - m_2^2} + \frac{g_2^*(q^2) f m f_2 m_2^2 f_2^* m_2^{*2}}{8m_c^2 (p^2 - m^2) (p'^2 - m_2^{*2})} \\ &\times \frac{m^2 + m_2^{*2} - q^2}{q^2 - m_2^2} + \dots \end{aligned} \quad (43)$$

The correlation function $\Pi^{\text{Phys}}(p, p')$ has simple Lorentz structure proportional to I, hence rhs of Eq. (43) is the corresponding invariant amplitude $\tilde{\Pi}^{\text{Phys}}(p^2, p'^2, q^2)$.

Using quark-gluon degrees of freedom, we can find the QCD side of the sum rule

$$\begin{aligned} \Pi^{\text{OPE}}(p, p') &= 2i^2 \int d^4x d^4y e^{ip'y} e^{-ipx} \\ &\left\{ \times \text{Tr} \left[\gamma_5 S_c^{ia}(y-x) \tilde{S}_c^{jb}(-x) \gamma_5 \tilde{S}_c^{bj}(x) S_c^{ai}(x-y) \right] \right. \\ &\left. + \text{Tr} \left[\gamma_5 S_c^{ib}(y-x) \tilde{S}_c^{ja}(-x) \gamma_5 \tilde{S}_c^{bj}(x) S_c^{ai}(x-y) \right] \right\}. \end{aligned} \quad (44)$$

The sum rule for the strong form factor $g_2(q^2)$ reads

$$\begin{aligned} g_2(q^2) &= \frac{8m_c^2}{f m f_2^2 m_2^4} \frac{q^2 - m_2^2}{m^2 + m_2^2 - q^2} \\ &\times e^{m^2/M_1^2} e^{m_2^2/M_2^2} \tilde{\Pi}(\mathbf{M}^2, \mathbf{s}_0, q^2), \end{aligned} \quad (45)$$

with $\tilde{\Pi}(\mathbf{M}^2, \mathbf{s}_0, q^2)$ being the invariant amplitude $\tilde{\Pi}^{\text{OPE}}(p^2, p'^2, q^2)$ corresponding to the correlator $\Pi^{\text{OPE}}(p, p')$ after the Borel transformations and subtractions. Numerical computations are carried out using Eq. (45), parameters of the meson η_c from Table I, and working regions for \mathbf{M}^2 and \mathbf{s}_0 . The Borel and continuum subtraction parameters M_1^2 and s_0 in the T_{4c} channel are chosen as in Eq. (13), whereas for M_2^2 and s'_0 which correspond to the η_c channel, we employ

$$M_2^2 \in [3.5, 4.5] \text{ GeV}^2, \quad s'_0 \in [11, 12] \text{ GeV}^2. \quad (46)$$

The interpolating function $\mathcal{G}_2(Q^2)$ has the following parameters: $\mathcal{G}_2^0 = 0.38 \text{ GeV}^{-1}$, $c_2^1 = 3.62$, and $c_2^2 = -4.17$. For the strong coupling g_2 , we get

$$g_2 \equiv \mathcal{G}_2(-m_2^2) = (1.7 \pm 0.4) \times 10^{-1} \text{ GeV}^{-1}. \quad (47)$$

The width of the process $T_{4c} \rightarrow \eta_c \eta_c$ is determined by means of the formula

$$\Gamma[T_{4c} \rightarrow \eta_c \eta_c] = g_2^2 \frac{m_2^2 \tilde{\lambda}}{8\pi} \left(1 + \frac{\tilde{\lambda}^2}{m_2^2} \right), \quad (48)$$

where $\tilde{\lambda} = \lambda(m, m_2, m_2)$. Finally, we obtain

$$\Gamma[T_{4c} \rightarrow \eta_c \eta_c] = (24 \pm 8) \text{ MeV}. \quad (49)$$

For the channel $T_{4c} \rightarrow \eta_c \eta_c(2S)$, we use

$$M_2^2 \in [3.5, 4.5] \text{ GeV}^2, \quad s'_0 \in [13, 14] \text{ GeV}^2, \quad (50)$$

and find

$$g_2^* \equiv \mathcal{G}_2^*(-m_2^2) = (9.0 \pm 2.8) \times 10^{-2} \text{ GeV}^{-1}. \quad (51)$$

The g_2^* is evaluated using the fit function $\mathcal{G}_2^*(Q^2)$ with the parameters $\mathcal{G}_2^{0*} = 0.21 \text{ GeV}^{-1}$, $c_2^{1*} = 3.62$, and $c_2^{2*} = -4.17$. The width of this decay is equal to

$$\Gamma[T_{4c} \rightarrow \eta_c \eta_c(2S)] = (5 \pm 2) \text{ MeV}. \quad (52)$$

Treatment of the P -wave process $T_{4c} \rightarrow \eta_c \chi_{c1}(P)$ does not generate additional technical details, and is performed in a usual manner. The three-point correlator to be considered in this case is

$$\begin{aligned} \Pi_\mu(p, p') &= i^2 \int d^4x d^4y e^{ip'y} e^{-ipx} \langle 0 | \mathcal{T} \{ J_\mu^{\chi_{c1}}(y) \\ &\times J^{\eta_c}(0) J^\dagger(x) \} | 0 \rangle, \end{aligned} \quad (53)$$

where $J_\mu^{\chi_{c1}}(y)$ is the interpolating current for the meson $\chi_{c1}(1P)$

$$J_\mu^{\chi_{c1}}(y) = \bar{c}_j(x) \gamma_5 \gamma_\mu c_j(y). \quad (54)$$

In terms of the physical parameters of involved particles the correlation function has the form

$$\begin{aligned} \Pi_\mu^{\text{Phys}}(p, p') &= g_3(q^2) \frac{f m f_2 m_2^2 f_3 m_3}{2m_c (p^2 - m^2) (p'^2 - m_3^2)} \\ &\times \frac{1}{q^2 - m_2^2} \left[\frac{m^2 - m_3^2 - q^2}{2m_3^2} p'_\mu - q_\mu \right] + \dots \end{aligned} \quad (55)$$

In Eq. (55) m_3 and f_3 are the mass and decay constant of the meson $\chi_{c1}(1P)$. To derive the correlator $\Pi_\mu^{\text{Phys}}(p, p')$, we have used the known matrix elements of the tetraquark X_{4c} and meson η_c , as well as new matrix elements

$$\langle 0 | J_\mu^{\chi_{c1}} | \chi_{c1}(p') \rangle = f_3 m_3 \varepsilon_\mu^*(p'), \quad (56)$$

and

$$\langle \eta_c(q) \chi_{c1}(p') | T_{4c}(p) \rangle = g_3(q^2) p \cdot \varepsilon^*(p'), \quad (57)$$

where $\varepsilon_\mu^*(p')$ is the polarization vector of $\chi_{c1}(1P)$.

The QCD side $\Pi_\mu^{\text{OPE}}(p, p')$ is given by the formula

$$\begin{aligned} \Pi_\mu^{\text{OPE}}(p, p') &= 2i \int d^4x d^4y e^{ip'y} e^{-ipx} \\ &\times \left\{ \text{Tr} \left[\gamma_\mu \gamma_5 S_c^{ia}(y-x) \tilde{S}_c^{jb}(-x) \gamma_5 \tilde{S}_c^{bj}(x) S_c^{ai}(x-y) \right] \right. \\ &\left. + \text{Tr} \left[\gamma_\mu \gamma_5 S_c^{ib}(y-x) \tilde{S}_c^{ja}(-x) \gamma_5 \tilde{S}_c^{bj}(x) S_c^{ai}(x-y) \right] \right\}. \end{aligned} \quad (58)$$

The sum rule for $g_3(q^2)$ is derived using invariant amplitudes corresponding to terms $\sim p'_\mu$ in $\Pi_\mu^{\text{Phys}}(p, p')$ and $\Pi_\mu^{\text{OPE}}(p, p')$.

In numerical analysis, the parameter M_2^2 and s'_0 in the χ_{c1} channel are chosen in the following way

$$M_2^2 \in [4, 5] \text{ GeV}^2, \quad s'_0 \in [13, 14] \text{ GeV}^2. \quad (59)$$

For the parameters of the fit function $\mathcal{G}_3(Q^2)$, we get $\mathcal{G}_3^0 = 5.16$, $c_3^1 = 3.16$, and $c_3^2 = -3.87$. Then, the strong coupling g_3 is equal to

$$g_3 \equiv \mathcal{G}_3(-m_2^2) = 2.5 \pm 0.6. \quad (60)$$

The width of the decay $X_{4c} \rightarrow \eta_c \chi_{c1}(P)$ can be calculated by mean of the expression

$$\Gamma[T_{4c} \rightarrow \eta_c \chi_{c1}(P)] = g_3^2 \frac{\hat{\lambda}^3}{24\pi m_3^2}, \quad (61)$$

where $\hat{\lambda} = \lambda(m, m_3, m_2)$. The width of this process is equal to

$$\Gamma[T_{4c} \rightarrow \eta_c \chi_{c1}(P)] = (12 \pm 4) \text{ MeV}. \quad (62)$$

The partial widths of five decays of the tetraquark T_{4c} are collected in Table II. Based on these results, it is not difficult to find that

$$\Gamma_{4c} = (112 \pm 21) \text{ MeV}. \quad (63)$$

V. WIDTH OF THE TETRAQUARK T_{4b}

In this section, we evaluate the width of the fully heavy tetraquark T_{4b} . Our analysis shows that T_{4b} is unstable

i	Channels	$g_i^{(*)} \times 10 \text{ (GeV}^{-1}\text{)}$	$\Gamma_i^{(*)} \text{ (MeV)}$
1	$T_{4c} \rightarrow J/\psi J/\psi$	5.1 ± 1.1	56 ± 18
1*	$T_{4c} \rightarrow J/\psi \psi'$	4.2 ± 1.0	15 ± 5
2	$T_{4c} \rightarrow \eta_c \eta_c$	1.7 ± 0.4	24 ± 8
2*	$T_{4c} \rightarrow \eta_c \eta_c(2S)$	0.9 ± 0.28	5 ± 2
3	$T_{4c} \rightarrow \eta_c \chi_{c1}(1P)$	$25 \pm 6^*$	12 ± 4
4	$T_{4b} \rightarrow \eta_b \eta_b$	1.9 ± 0.4	94 ± 28

TABLE II: Decay channels of the tetraquarks T_{4c} and T_{4b} , strong couplings $g_i^{(*)}$, and partial widths $\Gamma_i^{(*)}$. The coupling g_3 is dimensionless.

against strong decays and dissociates to mesons $\eta_b \eta_b$. Investigation of the decay $T_{4b} \rightarrow \eta_b \eta_b$ can be performed in accordance with a scheme utilized in the previous section to consider the process $T_{4c} \rightarrow \eta_c \eta_c$.

The correlation function necessary to extract a sum rule for the form factor $g_4(q^2)$ in this case is given by the expression

$$\begin{aligned} \Pi_b(p, p') &= i^2 \int d^4x d^4y e^{ip'y} e^{-ipx} \langle 0 | \mathcal{T} \{ J^{\eta_b}(y) \\ &\times J^{\eta_b}(0) J^\dagger(x) \} | 0 \rangle, \end{aligned} \quad (64)$$

where $J^{\eta_b}(x)$ is the interpolating current for the meson η_b

$$J^{\eta_b}(x) = \bar{b}_j(x) i \gamma_5 b_j(x). \quad (65)$$

To determine g_4 , we use the standard "ground-state+continuum" scheme. Then, it is not difficult to find the physical and QCD sides of the sum rule, which are given by the following expressions

$$\begin{aligned} \Pi_b^{\text{Phys}}(p, p') &= \frac{\langle 0 | J^{\eta_b} | \eta_b(p') \rangle \langle 0 | J^{\eta_b} | \eta_b(q) \rangle}{p'^2 - m_4^2} \frac{q^2 - m_4^2}{q^2 - m_4^2} \\ &\times \langle \eta_b(p') \eta_b(q) | T_{4b}(p) \rangle \frac{\langle T_{4b}(p) | J^\dagger | 0 \rangle}{p^2 - m^2} + \dots, \end{aligned} \quad (66)$$

where m_4 is the mass of the η_b meson. The matrix elements which are required to simplify $\Pi_b^{\text{Phys}}(p, p')$ have forms

$$\begin{aligned} \langle 0 | J^{\eta_b} | \eta_b \rangle &= \frac{f_4 m_4^2}{2m_b}, \\ \langle \eta_b(p') \eta_b(q) | T_{4b}(p) \rangle &= g_4(q^2) p \cdot p, \end{aligned} \quad (67)$$

where f_4 is the decay constant of η_b .

To find the QCD side of the sum rule $\Pi_b^{\text{OPE}}(p, p')$ one needs to replace all c -quark propagators in Eq. (44) by relevant $S_b(x)$ propagators. The sum rule for the coupling predicts

$$g_4 \equiv \mathcal{G}_4(-m_4^2) = (1.9 \pm 0.4) \times 10^{-1} \text{ GeV}^{-1}. \quad (68)$$

The coupling g_4 is calculated by means of the extrapolating function $\mathcal{G}_4(Q^2)$ with $\mathcal{G}_4^0 = 0.63$, $c_4^1 = 3.21$, and

$c_4^2 = -6.58$. In sum rule computations the parameters M_1^2 and s_0 in T_{4b} channel are chosen in accordance with Eq. (15), whereas for M_2^2 and s'_0 in the η_b channel, we employ

$$M_2^2 \in [10, 12] \text{ GeV}^2, \quad s'_0 \in [93, 97] \text{ GeV}^2. \quad (69)$$

Results obtained for $g_4(Q^2)$ and the function $\mathcal{G}_4(Q^2)$ are plotted in Fig. 5.

The width of the decay $T_{4b} \rightarrow \eta_b \eta_b$ can be found by means of the expression Eq. (48) with evident replacements. Our prediction reads

$$\Gamma[T_{4b} \rightarrow \eta_b \eta_b] = (94 \pm 28) \text{ MeV}. \quad (70)$$

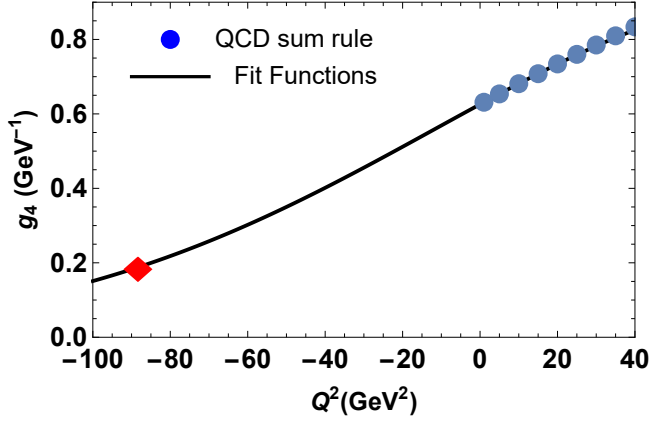


FIG. 5: The sum rule predictions and fit function for the strong coupling $g_4(Q^2)$.

VI. DISCUSSION AND CONCLUDING NOTES

We have explored the fully charmed and beauty tetraquarks T_{4c} and T_{4b} in the context of QCD sum rule method. We have modeled them as diquark-antidiquark systems composed of pseudoscalar ingredients. Predictions obtained in the current article for the mass $m = (6928 \pm 50) \text{ MeV}$ and width $\Gamma_{4c} = (112 \pm 21) \text{ MeV}$ of the fully charmed state T_{4c} allow us to confront them with available data of LHCb-ATLAS-CMS collaborations.

Data of interest, reported by these experiments are

$$\begin{aligned} m^{\text{LHCb}} &= (6905 \pm 11 \pm 7) \text{ MeV}, \\ \Gamma^{\text{LHCb}} &= (80 \pm 19 \pm 33) \text{ MeV}, \end{aligned} \quad (71)$$

$$\begin{aligned} m^{\text{ATL}} &= 6870 \pm 30^{+60}_{-10} \text{ MeV}, \\ \Gamma^{\text{ATL}} &= 120 \pm 40^{+30}_{-10} \text{ MeV}, \end{aligned} \quad (72)$$

and

$$\begin{aligned} m^{\text{CMS}} &= (6927 \pm 9 \pm 5) \text{ MeV}, \\ \Gamma^{\text{CMS}} &= (122 \pm 22 \pm 19) \text{ MeV}. \end{aligned} \quad (73)$$

It is evident, that the mass of the tetraquark T_{4c} is in excellent agreement with m^{CMS} , and is compatible with m^{LHCb} and m^{ATL} as well.

Comparing the width of T_{4c} with available data, one sees that within errors of calculations and measurements, Γ_{4c} is consistent with all of them. Therefore, by taking into account the mass of T_{4c} , we inclined to idea that this tetraquark is a nice candidate to the resonance $X(6900)$. Though, central values of Γ_{4c} and Γ^{CMS} , do not coincide, there exist a possibility to improve this agreement by including into consideration other decay mode(s) of T_{4c} . We would like to remind that in Ref. [20], we performed similar analysis for the fully charmed scalar diquark-antidiquark state X_{4c} with axial-vector constituents. The mass and width of X_{4c} allowed us to identify it with the resonance $X(6600)$.

Present investigations include detailed calculations of the both mass and width for the tetraquark T_{4c} . The LHCb-ATLAS-CMS resonances were explored in the frameworks of various models and methods. Our conclusions are in accord with the suggestion of Ref. [31] about the nature of $X(6900)$.

During last years, the fully beauty exotic mesons were also under intensive investigations. The tetraquark T_{4b} , which has been studied in this article, is a beauty counterpart of the fully charmed state T_{4c} . It turned out that T_{4b} is also unstable particle and can decay to $\eta_b \eta_b$ mesons. Its parameters may be interesting for future experimental studies of fully beauty resonances.

-
- [1] R. L. Jaffe, Phys. Rev. D **15**, 267 (1977).
 - [2] R. L. Jaffe, Phys. Rev. Lett. **38**, 195 (1977) Erratum: [Phys. Rev. Lett. **38**, 617 (1977)].
 - [3] J. P. Ader, J. M. Richard and P. Taxil, Phys. Rev. D **25**, 2370 (1982).
 - [4] H. J. Lipkin, Phys. Lett. B **172**, 242 (1986).
 - [5] S. Zouzou, B. Silvestre-Brac, C. Gignoux and J. M. Richard, Z. Phys. C **30**, 457 (1986).
 - [6] J. Carlson, L. Heller and J. A. Tjon, Phys. Rev. D **37**, 744 (1988).
 - [7] F. S. Navarra, M. Nielsen and S. H. Lee, Phys. Lett. B **649**, 166 (2007).
 - [8] M. Karliner and J. L. Rosner, Phys. Rev. Lett. **119**, 202001 (2017).
 - [9] E. J. Eichten and C. Quigg, Phys. Rev. Lett. **119**, 202002 (2017).
 - [10] Y. Xing, and R. Zhu, Phys. Rev. D **98**, 053005 (2018).
 - [11] S. S. Agaev, K. Azizi, B. Barsbay and H. Sundu, Phys. Rev. D **99**, 033002 (2019).
 - [12] G. Li, X. F. Wang, and Y. Xing, Eur. Phys. J. C **79**, 210

- (2019).
- [13] H. Sundu, S. S. Agaev and K. Azizi, *Eur. Phys. J. C* **79**, 753 (2019).
 - [14] S. S. Agaev, K. Azizi and H. Sundu, *Nucl. Phys. B* **951**, 114890 (2020).
 - [15] S. S. Agaev, K. Azizi, B. Barsbay, and H. Sundu, *Phys. Rev. D* **101**, 094026 (2020).
 - [16] S. S. Agaev, K. Azizi, B. Barsbay, and H. Sundu, *Eur. Phys. J. A* **56**, 177 (2020).
 - [17] S. S. Agaev, K. Azizi, B. Barsbay and H. Sundu, *Eur. Phys. J. A* **57**, 106 (2021).
 - [18] S. S. Agaev, K. Azizi, B. Barsbay and H. Sundu, *Chin. Phys. C* **45**, 013105 (2021).
 - [19] F. S. Yu, *Eur. Phys. J. C* **82**, 641 (2022).
 - [20] S. S. Agaev, K. Azizi, B. Barsbay and H. Sundu, *arXiv:2304.03244* [hep-ph].
 - [21] R. N. Faustov, V. O. Galkin, and E. M. Savchenko, *Symmetry* **14**, 2504 (2022).
 - [22] R. Aaij *et al.* [LHCb], *Phys. Lett. B* **707**, 52 (2012).
 - [23] V. Khachatryan *et al.* [CMS], *JHEP* **09**, 094 (2014).
 - [24] V. M. Abazov *et al.* [D0], *Phys. Rev. D* **90**, 111101 (2014).
 - [25] V. M. Abazov *et al.* [D0], *Phys. Rev. Lett.* **116**, 082002 (2016).
 - [26] V. Khachatryan *et al.* [CMS], *JHEP* **05**, 013 (2017).
 - [27] R. Aaij *et al.* [LHCb], *Sci. Bull.* **65**, 1983 (2020).
 - [28] E. Bouhova-Thacker [ATLAS], *PoS ICHEP2022*, 806 (2022).
 - [29] J. Zhang, *et al.* [CMS] *PoS ICHEP2022*, 775 (2022), *arXiv:2212.00504* [hep-ex].
 - [30] J. R. Zhang, *Phys. Rev. D* **103**, 014018 (2021).
 - [31] R. M. Albuquerque, S. Narison, A. Rabemananjara, D. Rabetiarivony and G. Randriamanatrika, *Phys. Rev. D* **102**, 094001 (2020).
 - [32] C. Becchi, A. Giachino, L. Maiani and E. Santopinto, *Phys. Lett. B* **806**, 135495 (2020).
 - [33] X. K. Dong, V. Baru, F. K. Guo, C. Hanhart and A. Nefediev, *Phys. Rev. Lett.* **126**, 132001 (2021). [erratum: *Phys. Rev. Lett.* **127**, 119901 (2021)].
 - [34] X. K. Dong, V. Baru, F. K. Guo, C. Hanhart, A. Nefediev and B. S. Zou, *Sci. Bull.* **66**, 2462 (2021).
 - [35] Z. R. Liang, X. Y. Wu and D. L. Yao, *Phys. Rev. D* **104**, 034034 (2021).
 - [36] Z. G. Wang, *Nucl. Phys. B* **985**, 115983 (2022).
 - [37] P. Niu, Z. Zhang, Q. Wang, and M. L. Du, *arXiv:2212.06535* [hep-ph].
 - [38] W. C. Dong, Z. G. Wang, *arXiv:2211.11989* [hep-ph].
 - [39] Z. R. Liang, X. Y. Wu and D. L. Yao, *arXiv:2212.14339* [hep-ph].
 - [40] S. Q. Kuang, Q. Zhou, D. Guo, Q. H. Yang, and L. Y. Dai, *arXiv:2302.03968* [hep-ph].
 - [41] M. A. Shifman, A. I. Vainshtein and V. I. Zakharov, *Nucl. Phys. B* **147**, 385 (1979).
 - [42] M. A. Shifman, A. I. Vainshtein and V. I. Zakharov, *Nucl. Phys. B* **147**, 448 (1979).
 - [43] S. S. Agaev, K. Azizi and H. Sundu, *Turk. J. Phys.* **44**, 95 (2020).
 - [44] R. L. Workman *et al.* [Particle Data Group], *Prog. Theor. Exp. Phys.* **2022**, 083C01 (2022).
 - [45] V. V. Kiselev, A. K. Likhoded, O. N. Pakhomova, and V. A. Saleev, *Phys. Rev. D* **65**, 034013 (2002).
 - [46] D. Hatton *et al.* [HPQCD], *Phys. Rev. D* **102**, 054511 (2020).
 - [47] D. Hatton, C. T. H. Davies, J. Koponen, G. P. Lepage, and A. T. Lytle, *Phys. Rev. D* **103**, 054512 (2021).
 - [48] E. Veli Veliev, K. Azizi, H. Sundu, and G. Kaya, *PoS (Confinement X) 339*, 2012; *arXiv:1205.5703* [hep-ph].